physical sciences forum

MDPI

Proceeding Paper

Introduction to a "Radical" Working Hypothesis about a Hemisphere-Scale Impact on Dione (Saturn) †

Balázs Bradák, Mayuko Nishikawa and Christopher Gomez *

Faculty of Oceanology, Kobe University, 5-1-1 Fukaeminami-machi, Higashinada-ku, Kobe 658-0022, Japan; e-mail1 (B.B.); e-mail2 (M.N.)

* Correspondence: bradak.b@port.kobe-u.ac.jp

† Presented at the 2nd Electronic Conference on Universe, 16 February–2 March 2023; Available online: https://ecu2023.sciforum.net/.

Abstract: The study introduces a theory about a giant impact on the surface of Dione. Our study suspects a relatively low-velocity (≤5 km/s) collision between a c.a. 50–80 km diameter object and Dione, which might result in resurfacing its Intermediate Cratered Terrain. The source of the impactor might be a unique satellite-centric debris, a unique impactor population, suspected in the Saturnian system. Other possible candidates are asteroid(s) appearing during the outer Solar System heavy bombardment period, or a collision, which might happen during the "giant impact phase" in the early Saturnian system (coinciding with the Late Heavy Bombardment, or not).

Keywords: Dione; Saturn; icy satellite; giant impact theory; resurfacing

Citation: Bradák, B.; Nishikawa, M.; Gomez, C. Introduction to a "Radical" Working Hypothesis about a Hemisphere-Scale Impact on Dione (Saturn). *Phys. Sci. Forum* **2023**, *3*, x. https://doi.org/10.3390/xxxxx

Published: 15 February 2023

Copyright: © 2023 by the authors. Submitted for possible open access publication under the terms and conditions of the Creative Commons Attribution (CC BY) license (https://creativecommons.org/licenses/by/4.0/).

1. Introduction

The target of the study is Dione, one of Saturn`s satellites, and its surface characteristics, especially with a focus on the possible relationship between the distribution pattern of certain size craters and resurfacing processes. The pivot of the study is the region, located westward from the Eurotas and Palatine chasmata (Faulted Terrain), defined as one of the Intermediate Cratered Terrains (ICTs) [1]. Chronologically Intermediate Cratered Terrain might form between, (or following) the formation of the two oldest terrains (so-called Dense Cratered Terrain, DCT 1 and 2; both c.a. 4.1 Ga), during the expected outer Solar System heavy bombardment period (independently from its spike-like or steady decline nature) (3.5 +1.0/−2.6 Ga) [1]. Kirchoff and Schenk [1] suggest that the region resurfaced at some point through a still unknown process, which erased all the previous craters. Some theories have been built to explain such process, including burial by material "snowing" down from the ring [2,3], thermal activity from tidal dissipation [4–8], and subsequent formation of larger (D ≥ 50 km) craters and their ejecta blanket [1].

We propose a working hypothesis that suggests a hemisphere-scale impact or collision as an alternative cause and trigger of surface renewal processes. The goal of our research is to support or deny such a hypothesis by the study of crater distribution patterns in Dione (with a focus on one of the ITCs) which may indicate the appearance of secondary crater formation related to the putative impact.

2. Data and Methods

2.1. Calculations Supporting the Estimation of the Primary Impactor and Secondary Crater Size

The transient crater size (D_t, km) is determined from the observed crater size (D, km) [9,10]:

$$D = 0.7Dt^{1.13} \quad (1)$$

The size of the primary impactor (d, km) is derived from D_t [9]:

$$Dt = 1.1\left(\frac{vi^2}{g}\right)^{0.217}\left(\frac{\rho i \sin\alpha}{\rho t}\right)^{0.333} d^{0.783} \quad (2)$$

where d is the impactor diameter in km with a density ϱ_i (0.6 g/cm3; [10]), velocity v_i (in the original study—U; for detailed information please see Section 2.1.1), and incidence angle α (for detailed information please see Section 2.1.1). ϱt is the density of the icy crust (910 kg/m^3), and g is the acceleration of gravity in km/s^2 at the target surface, which is 2.32 × 10^{-4} km/s^2 in the case of Dione.

The average size of the secondary impactors is determined by the following [11]:

$$l_{AVG} = \frac{T}{\rho_t {v_e}^{2/3} {v_i}^{4/3}} d \quad (3)$$

where l_{AVG} is the average size (m) of the ejected fragments, and T is the tension fracture, equal to 0.17 × 108 Pa in ice [12]. As it is described in the previous equations, d is the size of the impactor (km), ϱ_t is the density of the ice at the target location: 0.91 g/cm^3 [10], v_e is the speed of the ejecta (for "rubble ejecta": 1.98 km/s; [10]), and v_i is the velocity of the impactor (please see detailed information in Section 2.21).

The maximum size of the secondary projectiles was derived from l_{AVG} [11]:

$$l_{MAX} = \frac{m_W+3}{2} l_{AVG} \quad (4)$$

where l_{MAX} is the maximum size (m) of the ejected fragments, l_{AVG} is the average fragment size (m), and mW is the so-called Weibulls constant, 8.7 for ice [12].

The ejected mass (M_{tot}; kg) in the case of the theoretical impact (if a secondary crater ring or any pattern is found, and the original impactor/impact crater size can be estimated) is calculated by

$$M_{tot} = 3.75 \times 10^{-2} \varrho_t D_t^3 \quad (5)$$

where D_t is the transient crater diameter of the putative crater in km, indicated by the secondary craters, and ϱ_t is the density of the ice at the target location: 0.91 g/cm^3 [10].

2.1.1. Scenarios of the Secondary Crater Formation

To determine the characteristic of the impact causing hemisphere scale renewal, the size variation of secondary craters was simulated as a result of various size impactors. As it was already indicated above, two variables were used during the simulation, the speed of the impactor and the impact angle. A set of impact velocities, including 3.93, 5.81 and 7.69 km/s, and 20.4 km/s was used. The former three represent the collision velocity calculated for Main Asteroid Belt collisions [13], and the latter was applied in the various studies targeting asteroid impact reconstructions in icy planetary bodies [9,10]. As a second variable, two different impact angles were set, one is the average, commonly applied 45° [9,10], and a relatively low, 20° incidence angle, which appears in a certain study, modeling low-angle impacts and their effects on planetary surfaces [14].

2.2. The Studied Location and the Crater Distribution Map

The studied region, one of the so-called Intermediate Cratered Terrains [1] is spreading approximately between latitude 50° and −50° and longitude c.a. 300° to 60° (westward) (Figure 1). The source of the map of Dione is based on Cassini—Voyager Global Mosaic 154 m v1 map, can be found at Astropedia—Lunar and Planetary Cartographic Catalog [15–18]. The applied nomenclature follows the recommendation of the Gazetteer of Planetary Nomenclature [19].

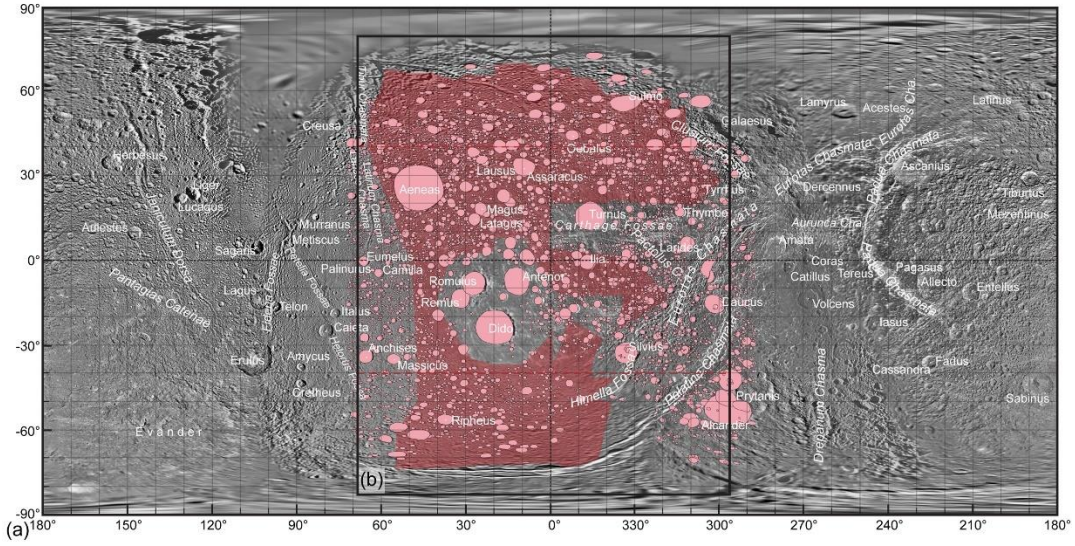

Figure 1. (**a**) Cassini-Voyager Global Mosaic 154 m v1 map. (**b**) the region of study, consisting of the ICT (red, transparent polygon) [1]. The ⌀ ≥ 4 km craters, used in the analysis are indicated by pink ellipsoids. Dashed red lines: areas with crater mapping uncertainties (see Section 2.2).

The remote sensing and GIS research was performed by QGIS 3.22 software. In previous studies, the mapping of craters in Dione was limited to craters with ⌀ ≥ 4 km crater diameter due to problems during the identification of smaller craters in image mosaics with lower resolution [1]. To avoid the increasing bias in the results due to the use of barely identifiable smaller craters, this study also applies such a criterion. Over 8800 craters fulfilling the minimum ⌀ ≥ 4 km size limit were identified, including about 5400 craters found in the studied area (Figure 1b). The crater distribution maps were created by using the centroids of the craters and a grid with a 100 km × 100 km basic cell size, overlapping the map. The distribution map is based on the number of certain-size craters, appearing in the cells of the grid (Figure 2).

Please note, that the crater mapping had some limitations in certain areas located between latitude 40° to 90° and especially between −40° to −90° due to the quality of the image mosaics and the distortion of the map. This limitation may bias the results and therefore the areas with such potential uncertainty marked by dashed red lines in Figure 1b and the maps of Figure 2.

3. Results and Discussion

3.1. Simulation of Secondary Crater Formation

Comparing the eight scenarios based on various impact and collision velocities and angles (Scen. 1 to 8; Table 1), the main results can be summarized as followings:

The change in impact angle from the commonly applied 45° [9,10] to a low, 20° incidence angle [14] does not significantly influence the secondary crater size.

The increasing collision velocity significantly decreases the size of ejectiles and thus the size of secondary craters. In high impact velocity, the secondary crater size would barely reach 1 km even in the case of a relatively big impactor (Scen. 4 and 8; Table 1). It suggests that even if a larger impact happened if the velocity was higher (c.a. >10 m/s) the secondary craters would blend in the mass of similar size, common primary craters.

The minimum crater size requirement seems to limit the further interpretation of the results, i.e., ⌀ < 4 km secondary craters may be formed by large impacts, but they were not mapped due to the uncertainty during their identification.

In a summary, crater distribution patterns observed in this study can indicate relatively low velocity, "asteroid belt-like" collisions between Dione and a minimum c.a. ⌀ 30–40 km impactor (resulting in a minimum c.a. ⌀ 200–250 km primary craters).

Table 1. Relationship between the primary impactor and secondary crater formation on Dione. Columns 1 to 8 shows various scenarios, using various combination of impact velocity (U or vi) and angles (ψ), such as 1 (vi: 3.93 km/s; ψ: 20°), 2 (vi: 5.81 km/s; ψ: 20°), 3 (vi: 7.69 km/s; ψ: 20°), 4 (vi: 20.4 km/s; ψ: 20°), 5 (vi: 3.93 km/s; ψ: 45°), 6 (vi: 5.81 km/s; ψ: 45°), 7 (vi: 7.69 km/s; ψ: 45°), and 8 (vi: 20.4 km/s; ψ: 45°). Bold data: primary impactor size; red data: primary impacts which result in ⌀ < 4 km secondary craters; grey background: collision scenarios that might happen in the early history of Dione (based on the crater distribution results, see Section 3.2).

Crater Size [km]	Simulations (Impactor Size [km] | Secondary Crater Size [km])															
	Scen. 1		Scen. 2		Scen. 3		Scen. 4		Scen. 5		Scen. 6		Scen. 7		Scen. 8	
62 (Remus)	**8.0**	0.9	**6.5**	0.5	**5.5**	0.4	**3.2**	0.1	**8.3**	0.9	**6.7**	0.5	**5.7**	0.4	**3.3**	0.1
81 (Antenor)	**10.9**	1.3	**8.8**	0.7	**7.5**	0.5	**4.4**	0.1	**11.2**	1.3	**9.0**	0.7	**7.7**	0.5	**4.5**	0.1
90.1 (Romulus)	**12.3**	1.4	**9.9**	0.8	**8.5**	0.5	**4.9**	0.1	**12.6**	1.4	**10.2**	0.8	**8.7**	0.5	**5.1**	0.1
100	**13.8**	1.6	**11.1**	0.9	**9.5**	0.6	**5.5**	0.1	**14.2**	1.6	**11.4**	0.9	**9.8**	0.6	**5.7**	0.1
122 (Dido)	**17.3**	2.0	**13.9**	1.1	**11.9**	0.8	**6.9**	0.2	**17.8**	2.0	**14.3**	1.1	**12.3**	0.8	**7.1**	0.2
150	**21.8**	2.9	**17.6**	1.6	**15.0**	1.1	**8.8**	0.3	**22.5**	2.9	**18.1**	1.6	**15.5**	1.1	**9.0**	0.3
200	**30.2**	4.0	**24.3**	2.3	**20.8**	1.5	**12.1**	0.4	**31.1**	4.0	**25.0**	2.3	**21.4**	1.5	**12.5**	0.4
250	**38.9**	5.2	**31.3**	2.9	**26.8**	1.9	**15.6**	0.5	**40.0**	5.2	**32.2**	2.9	**27.6**	2.0	**16.1**	0.5
300	**47.7**	6.3	**38.4**	3.6	**32.9**	2.4	**19.2**	0.6	**49.2**	6.4	**39.6**	3.6	**33.9**	2.4	**19.7**	0.6
350	**56.8**	7.5	**45.8**	4.3	**39.2**	2.8	**22.8**	0.7	**58.6**	7.6	**47.1**	4.3	**40.4**	2.9	**23.5**	0.7
400	**66.1**	8.8	**53.2**	5.0	**45.6**	3.3	**26.5**	0.8	**68.1**	8.8	**54.8**	5.0	**46.9**	3.3	**27.3**	0.8
450	**75.5**	10.0	**60.8**	5.7	**52.0**	3.8	**30.3**	0.9	**77.8**	10.1	**62.6**	5.7	**53.6**	3.8	**31.2**	0.9
500	**85.0**	11.3	**68.5**	6.4	**58.6**	4.3	**34.1**	1.0	**87.6**	11.4	**70.5**	6.4	**60.4**	4.3	**35.2**	1.0
550	**94.7**	12.6	**76.3**	7.1	**65.3**	4.7	**38.0**	1.1	**97.6**	12.7	**78.5**	7.2	**67.3**	4.8	**39.2**	1.2

3.2. Distribution Patterns of Various Crater Classes

The distribution pattern of craters falling in four different diameter size classes was studied and compared to the general distribution pattern (all ⌀ ≥ 4 km craters; Figure 2a).

The pattern of the ⌀ 4–5.9 km crater class is similar to the general distribution, suggesting that even if there is some pattern it melts into the general crater allocation (Figure 2b).

The fragments of two concentric rings were identified in the distribution map of the ⌀ 6–7.9 km crater class (Figure 2c). An inner one at the edge of the relatively crater-clean area, named RLCT (Recent Large Crater Terrain), and an outer one roughly around latitude 30° (Figure 2c,f). The inner ring may be the result of impacts forming the larger craters in the area, such as Dido, Romulus, and Remus. The outer ring, if it is created by a putative impact, may be the result of a low angle collision (20°) with a c.a. ⌀ 48–57 km, relatively low-velocity (Scen. 1), or bigger, ⌀ 69–75 km and faster object (Scen. 2). Similar ring may form, if a bigger, ⌀ 49–59 km (Scen. 4), or ⌀ 71–79 km object (Scen. 5), collides with the same speeds (3.93 and 5.81 km/s, respectively), but at a greater impact angle (45°) (Table 1).

The distributions pattern of the craters falling into the ⌀ 8–9.9 km and the ⌀ 10–11.9 km crater classes are similar, they consist of some "randomly" located crater groups in the studied area, without any convincing pattern (Figure 2d,e).

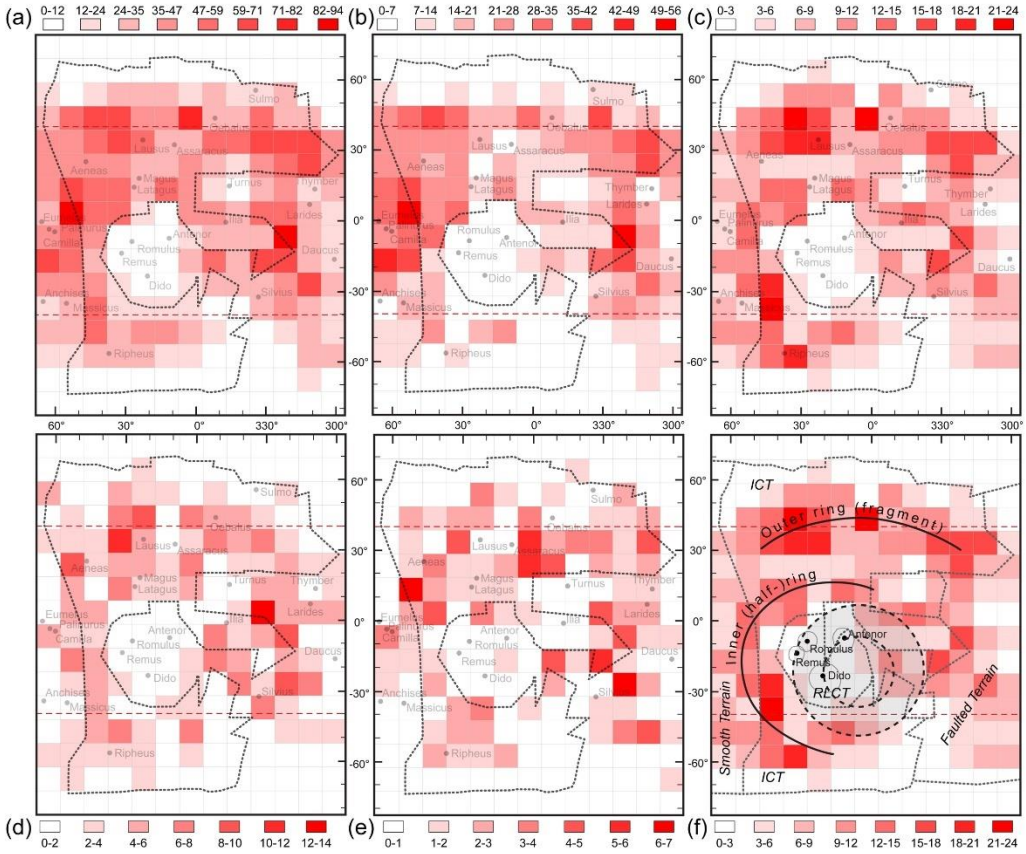

Figure 2. Crater distribution map of (**a**) all ⌀ ≥ 4 km craters; (**b**) ⌀ 4–5.9 km craters; (**c**) ⌀ 6–7.9 km craters; (**d**) ⌀ 8–9.9 km craters; (**e**) ⌀ 10–11.9 km craters. The dashed red lines: crater mapping uncertainties. The dotted black line (**a**–**e**): margin of *ICT* and other terrains (**f**). The cell size of the light grey grid is 100 × 100 km. Abbreviations: *ICT*—Intermediate Cratered Terrain, *RLCT*—Recent Large Crater Terrain. The grey area with black, dashed margins indicates the location of the putative impact crater (inner circle—⌀ 300 km; outer circle—⌀ 550 km).

3.3. Surface renewal Model for the Studied Intermediate Cratered Terrain

Kirchoff and Schenk [1] suggested that one possible explanation for the renewal of the surface in the ICT region is the results of impactors and their ejecta creating the ⌀ ≥ 50 km impact craters. Our working theory suggests that such impactors may be accompanied by a much bigger size, c.a. ⌀ 50–80 km impactor, resulting in forming a ⌀ 300–350 to ⌀ 500–550 km crater (Figure 3). During the excavation phase of such collision, 3.3–5.5 × 10^5 t (⌀ 300–350 km crater) to 1.3–1.7 × 10^6 t (⌀ 500–550 km crater) of debris might eject in the space, and return to the surface, covering large areas of the ICT with ejecta blanket (Figure 3b,c).

In addition to the ejecta blanket, in the case of low-angle collision, the sliding and ricocheting ejectiles [14] might cause surface planning by "plowing" and partial melts.

Following the excavation phase of the impact, such a size impactor may cause the uplift of the ice crust (rebound) and the rise of a subsurface diapir-like structure, made by the convective ice layer and/or the cryo-slurry at the center of the impact crater during the modification stage of the impact (Figure 3d,e). The diapir and central peak formed in the convective ice crust might later retreat due to isostatic relaxation of the surface. Diapir formation may cause the intensification of cryotectonic and cryovolcanic activity in the region, accompanied by faulting and cryo-slurry outflows. Such secondary processes might have a significant role in the surface renewal of ICT (Figure 3d,e).

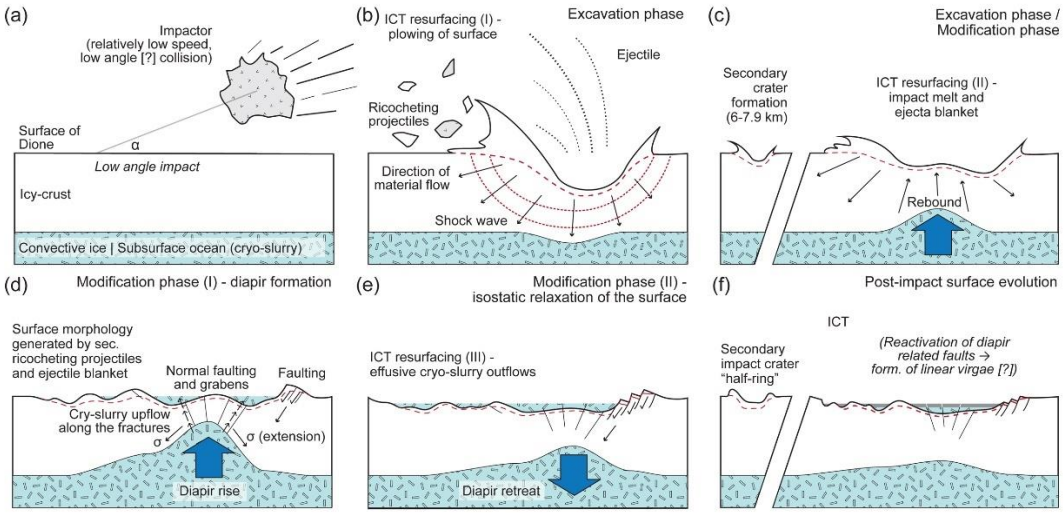

Figure 3. The surface main steps of surface renewal of Intermediate Cratered Terrain, following the asteroid impact. (**a**) low angle collision; (**b**) Excavation phase of impact and the "plowing" of the ICT`s surface; (**c**) Excavation/Modification phase transition and the ongoing deposition of ejecta blanket; (**d**,**e**) Modification phase with diapir formation and intensification of cryotectonic and cryovolcanic activity; and (**f**) post-impact surface evolution.

Here we introduced a working theory about a giant impact on the surface of Dione, which might contribute to the resurfacing of ICT, a region with unrevealed astrogeological history. Our putative impactor might be originated from a unique impactor population, suspected in the Saturnian system [20], or appeared during the outer Solar System heavy bombardment period, or during the so-called "giant impact phase" (c.a., 4 Ga; coinciding with the Late Heavy Bombardment or not), a period leaving middle-size satellite remnants, such as Dione, behind [21].

Given the results of the study, after all the hypothesis does not sound as "radical" as "dramatic" the title of our study. Future research aims more simulations about the effect of a giant impactor on the surface of Dione and possible astrogeological mapping and comparison of the surroundings of the putative impact and Evander crater, Dione`s largest impact crater, with a similar size to the estimated size range of our theoretical crater.

Author Contributions: Conceptualization, B.B.; methodology, B.B. and C.G.; formal analysis, B.B., N.M.; investigation, B.B.; writing—original draft preparation, B.B.; writing—review and editing, B.B. All authors have read and agreed to the published version of the manuscript.

Funding: This research received no external funding.

Institutional Review Board Statement:

Informed Consent Statement: Not applicable.

Data Availability Statement: Data will be provided via email upon request.

Acknowledgments:

Conflicts of Interest: The authors declare no conflict of interest.

References

1. Kirchoff, M.R.; Schenk, P. Dione's resurfacing history as determined from a global impact crater database. *Icarus* **2015**, *256*, 78–89. https://doi.org/10.1016/j.icarus.2015.04.010.
2. Kirchoff, M.R.; Schenk, P. Crater modification and geologic activity in Enceladus' heavily cratered plains: Evidence from the impact crater distribution. *Icarus* **2009**, *202*, 656–668. https://doi.org/10.1016/j.icarus.2009.03.034.
3. Schenk, P.; Hamilton, D.P.; Johnson, R.E.; McKinnon, W.B.; Paranicas, C.; Schmidt, J.; Showalter, M.R. Plasma, plumes and rings: Saturn system dynamics as recorded in global color patterns on its midsize icy satellites. *Icarus* **2011**, *211*, 740–757. https://doi.org/10.1016/j.icarus.2010.08.016.

4. Segatz, M.; Spohn, T.; Ross, M.; Schubert, G. Tidal dissipation, surface heat flow, and figure of viscoelastic models of Io. *Icarus* **1988**, *75*, 187–206. https://doi.org/10.1016/0019-1035(88)90001-2.
5. Chen, E.M.A.; Nimmo, F. Implications from Ithaca Chasma for the thermal and orbital history of Tethys. *Geophys. Res. Lett.* **2008**, *35*, L19203. https://doi.org/10.1029/2008GL035402.
6. Meyer, J.; Wisdom, J. Tidal evolution of Mimas, Enceladus, and Dione. *Icarus* **2008**, *193*, 213–223. https://doi.org/10.1016/j.icarus.2007.09.008.
7. Zhang, K.; Nimmo, F. Recent orbital evolution and the internal structures of Enceladus and Dione. *Icarus* **2009**, *204*, 597–609. https://doi.org/10.1016/j.icarus.2009.07.007.
8. Hammond, N.; Phillips, C.; Nimmo, F.; Kattenhorn, S. Flexure on Dione: Investigating subsurface structure and thermal history. *Icarus* **2013**, *223*, 418–422. https://doi.org/10.1016/j.icarus.2012.12.021.
9. Alvarellos, J.L.; Zahnle, K.J.; Dobrovolskis, A.R.; Hamill, P. Fates of satellite ejecta in the Saturn system. *Icarus* **2005**, *178*, 104–123. https://doi.org/10.1016/j.icarus.2005.04.017.
10. Alvarellos, J.L.; Dobrovolskis, A.R.; Zahnle, K.J.; Hamill, P.; Dones, L.; Robbins, S. Fates of satellite ejecta in the Saturn system, II. *Icarus* **2017**, *284*, 70–89. https://doi.org/10.1016/j.icarus.2016.10.028.
11. Mileikowsky, C.; Cucinotta, F.A.; Wilson, J.W.; Gladman, B.; Horneck, G.; Lindegren, L.; Melosh, J.; Rickman, H.; Valtonen, M.; Zheng, J.Q. Natural Transfer of Viable Microbes in Space: 1. From Mars to Earth and Earth to Mars. *Icarus* **2000**, *145*, 391–427. https://doi.org/10.1006/icar.1999.6317.
12. Melosh, H. Impact ejection, spallation, and the origin of meteorites. *Icarus* **1984**, *59*, 234–260. https://doi.org/10.1016/0019-1035(84)90026-5.
13. Farinella, P.; Davis, D.R. Collision rates and impact velocities in the main asteroid belt. *Icarus* **1992**, *97*, 111–123. https://doi.org/10.1016/0019-1035(92)90060-K.
14. Elbeshausen, D.; Wünnemann, K.; Collins, G.S. The transition from circular to elliptical impact craters. *J. Geophys. Res. Planets* **2013**, *118*, 2295–2309. https://doi.org/10.1002/2013JE004477.
15. Batson, R. *Voyager 1 and 2 Atlas of Six Saturnian Satellites (NASA-SP-474)*; National Aeronautics and Space Administration (NASA): Washington, DC, USA, 1984. Available online: https://ntrs.nasa.gov/archive/nasa/casi.ntrs.nasa.gov/19840027171.pdf (accessed on).
16. Greely, R.; Batson, R. *Planetary Mapping*; Cambridge University Press. New York, NY, USA, 2007; 312p, ISBN 0-521-30774-0.
17. Roatsch, T.; Kersten, E.; Matz, K.D.; Scholten, F.; Wagner, R.; Porco, C. Cartography of the Medium-Sized Saturnian Satellites Based on Cassini-ISS Images. Presented at the Enceladus and the Icy Moons of Saturn Conference, Lunar and Planetary Institute, Boulder, CO, USA, 26–29 July 2016. Available online: https://www.hou.usra.edu/meetings/enceladus2016/pdf/3032.pdf (accessed on).
18. Schneck, P. Global Color and Cartographic Mapping of Saturn's Midsize Icy Moons. Presented at the Enceladus and the Icy Moons of Saturn Conference, Lunar and Planetary Institute, Boulder, CO, USA, 26–29 July 2016. Available online: https://www.hou.usra.edu/meetings/enceladus2016/pdf/3053.pdf (accessed on).
19. Gazetteer of Planetary Nomenclature. International Astronomical Union (IAU), Working Group for Planetary System Nomenclature (WGPSN). Available online: https://asc-planetarynames-data.s3.us-west-2.amazonaws.com/dione_comp.pdf (accessed on 11 December 2022).
20. Ferguson, S.N.; Rhoden, A.R.; Kirchoff, M.R.; Salmon, J.J. A unique Saturnian impactor population from elliptical craters. *Earth Planet. Sci. Lett.* **2022**, *593*, 117652 https://doi.org/10.1016/j.epsl.2022.117652.
21. Asphaug, E.; Reufer, A. Late origin of the Saturn system. *Icarus* **2013**, *223*, 544–565. https://doi.org/10.1016/j.icarus.2012.12.009.

Disclaimer/Publisher's Note: The statements, opinions and data contained in all publications are solely those of the individual author(s) and contributor(s) and not of MDPI and/or the editor(s). MDPI and/or the editor(s) disclaim responsibility for any injury to people or property resulting from any ideas, methods, instructions or products referred to in the content.